

available at www.sciencedirect.comjournal homepage: www.elsevier.com/locate/chnjc

Article

Epoxidation of vinyl functionalized cubic $Ia3d$ mesoporous silica for immobilization of penicillin G acylase

Wangcheng Zhan, Yongjun Lü, Ling Yang, Yanglong Guo, Yanqin Wang, Yun Guo, Guanzhong Lu*

Key Laboratory for Advanced Materials, Research Institute of Industrial Catalysis, East China University of Science and Technology, Shanghai 200237, China



ARTICLE INFO

Article history:

Received 24 March 2014

Accepted 15 April 2014

Published 20 October 2014

Keywords:

Co-condensation method

Mesoporous silica

Enzyme

Immobilization

Penicillin G acylase

ABSTRACT

Epoxy functionalized cubic $Ia3d$ mesoporous silica (CIMS) was successfully synthesized by epoxidizing vinyl groups prepared on the CIMS by a co-condensation method. The synthesized material was characterized by X-ray diffraction, nitrogen sorption, transmission electron microscopy, thermogravimetric analysis, and solid state ^{13}C NMR. The vinyl groups were found to be easily epoxidized to yield epoxy functionalized CIMS. The epoxy functionalized CIMS was used as a support for the immobilization of penicillin G acylase (PGA), and the effects of the epoxy group on the initial activity and the operational stability of the immobilized PGA were studied. The results showed that the enzyme loading and initial activity of the immobilized PGA decreased with increasing amounts of epoxy groups. These observations were due to a decrease in the pore size of the mesoporous silica as well as an increase in the hydrophobicity of the silica surface. However, an appropriate amount of epoxy groups on the CIMS support was found to improve the operational stability of the immobilized PGA. This improvement was the result of increased interactions between the epoxy functionalized CIMS support and the PGA.

© 2014, Dalian Institute of Chemical Physics, Chinese Academy of Sciences.

Published by Elsevier B.V. All rights reserved.

1. Introduction

Enzymes are excellent catalysts with high chemo-, regio-, stereo-, and chiral-selectivity under mild conditions. However, their strong sensitivity to temperature, high cost, and difficulty in recovering active enzyme for reuse currently limit their industrial application [1,2]. Immobilization of enzymes can overcome these disadvantages, and many kinds of supports have been studied [3–7]. Owing to its highly ordered pore structure, large tunable pore diameter, high pore volume, and narrow pore size distribution, ordered mesoporous silica is a widely applicable support for the immobilization of enzymes

and can achieve a high activity per unit volume [8–12]. However, interaction between enzymes and ordered mesoporous silica is very weak, and the enzymes can be easily washed off during the catalytic process, resulting in poor operational stability [13]. Functionalization of the surface of mesoporous silica with organic groups can enhance its interaction with enzymes [14–17].

Post-synthesis grafting and co-condensation are currently the most common methods for functionalizing the surface of mesoporous silica with organic groups [18–21]. Compared with co-condensation, post-synthesis grafting has many disadvantages [22], such as the nonuniform distribution of the or-

*Corresponding author. Tel/Fax: +86-21-64252923; E-mail: gzhlu@ecust.edu.cn

This work was supported by the National Natural Science Foundation of China (21103048), the Program for New Century Excellent Talents in University (NCET-09-0343), and Shuguang Project of Shanghai Municipal Education Commission and Shanghai Education Development Foundation (10SG30).

DOI: 10.1016/S1872-2067(14)60156-X | <http://www.sciencedirect.com/science/journal/18722067> | Chin. J. Catal., Vol. 35, No. 10, October 2014

ganic groups created on the surface of the mesoporous silica. A large proportion of these organic groups appear on the external surface of the mesoporous silica or inside channels but near the channel openings [5]. Furthermore, the pore size and pore volume of the mesoporous silica, which greatly impact the activity of an immobilized enzyme [23–25], may be substantially decreased after post-synthesis grafting [26]. In contrast, the co-condensation method can be used to functionalize the surface of mesoporous silica in a single step via copolymerization of an organosilane with the silica precursor in the presence of a surfactant template [27–30]. This method results in a highly homogeneous distribution of the organic groups on the surface of the mesoporous silica [31,32].

Epoxy functionalized supports can immobilize enzymes through reaction between epoxy groups and the amino groups (NH_2^-) of the enzymes under mild conditions [33–36]. However, the conditions used to synthesize ordered mesoporous silica are usually strongly acidic, and epoxy groups cannot exist under such severe conditions, making co-condensation impossible. However, vinyl functionalized ordered mesoporous silica is easily synthesized by co-condensation [37–39], and the vinyl groups can be easily epoxidized [40,41]. This method enables epoxy groups to be uniformly distributed on the surface of mesoporous silica.

Cubic *Ia3d* mesoporous silica (CIMS) has recently received great attention owing to its large uniform pores (5–12 nm) and 3D interpenetrating bicontinuous networks of channels, which allow easy accessibility and fast transport of molecules [42–44]. Thus, enzymes immobilized on CIMS can achieve a high activity. However, the epoxidation of vinyl functionalized CIMS and its subsequent application to the immobilization of enzymes have not previously been reported.

In this paper, vinyl functionalized CIMS was synthesized by a co-condensation method and then epoxidized, and the epoxy functionalized CIMS was used as a support for the immobilization of penicillin G acylase (PGA). The influence of the epoxy groups on the initial activity and the operational stability of the immobilized PGA biocatalysts were studied.

2. Experimental

2.1. Chemicals

Non-ionic triblock copolymer P123 (EO20PO70EO20, MW = 5800, Aldrich), tetraethyl orthosilicate (TEOS), *m*-chloroperbenzoic acid (*m*-CPBA, 50%–55%, Alpha-Aesar), and vinyl triethoxysilane (VTES; Haida, China) were used in this work. PGA (804 U/mL) was purchased from Hiader Co. Ltd, Zhejiang, China. Penicillin G potassium salt was purchased from Shandong Lukang Pharmaceutical Co. Ltd., China. NaOH solution and phosphate buffer were prepared according to the literature [45]. *m*-CPBA was dried with anhydrous magnesium sulfate (MgSO_4). *m*-CPBA (2 g) and MgSO_4 (4 g) were added to 100 mL dichloromethane, after which the mixture was stirred to completely remove the water from the solution and then filtered. The concentration of *m*-CPBA in the dichloromethane was about 0.02 g/mL. All other chemicals were analytical grade and

were used as received.

2.2. Synthesis of vinyl functionalized CIMS (V-CIMS)

As-synthesized V-CIMS was prepared according to the literature [38]. P123 (5.68 g) and Na_2SO_4 (11.36 g) were dissolved in 160 mL of HCl (1 mol/L), and the mixture was stirred at 35 °C for 4 h. Then, 53.2 mmol of TEOS and 5–20 wt% VTES was added slowly under stirring. After continuous stirring at 35 °C for 24 h, the synthesis solution was transferred into a polypropylene bottle and crystallized at 100 °C for 24 h. The as-synthesized V-CIMS product was collected by filtration and dried overnight at 100 °C.

The P123 template was removed from the as-synthesized V-CIMS by extraction [46–48]. The as-synthesized V-CIMS (1.0 g) was mixed with 50 mL of 60 wt% H_2SO_4 solution, and the mixture was stirred at 95 °C for 24 h. The product was collected by filtration, washed successively with water and ethanol, and dried at 90 °C for 24 h under vacuum. The prepared samples were named V-CIMS(5%–20%), where the number in the bracket was the mass percent of VTES in the silica precursor.

2.3. Epoxidation of V-CIMS

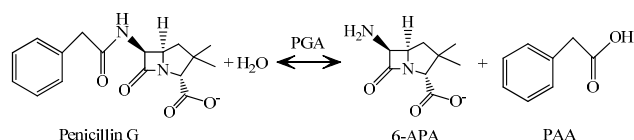
The epoxidation of V-CIMS was carried out at 35 °C in dichloromethane. V-CIMS (0.5 g) was mixed with 50 mL of the dichloromethane solution with *m*-CPBA, and the mixture was refluxed at 35 °C for 72 h under stirring. The resulting epoxy functionalized product, named E-CIMS(5%–20%), was collected by filtration, washed three times with dichloromethane, and dried under vacuum for 24 h.

2.4. Immobilization of PGA on E-CIMS supports

The E-CIMS support (0.1 g) was added to 5 mL of the enzyme solution (PGA, 804 U/mL) diluted with 0.1 mol/L of pH = 7.8 phosphate buffer ($V_{\text{enzyme}}/V_{\text{buffer}} = 1/4$). The mixture was shaken at 30 °C for 24 h at 130 rpm. The immobilized PGA was then filtered and washed with de-ionized water and buffer, after which the wet immobilized enzyme (IME) was ready for initial activity and operational stability testing.

2.5. Initial activity and operational stability tests

The enzyme activity of the immobilized PGA was evaluated by titrating phenylacetic acid (PAA), a by-product in the hydrolysis reaction of penicillin G potassium salt (Scheme 1). The formation of PAA lowers the pH of the hydrolysis mixture solution. The activity of PGA can be determined by titrating the produced PAA with NaOH solution until the initial pH of the



Scheme 1. Hydrolysis of penicillin G catalyzed by penicillin G acylase (PGA).

reaction solution is reached. The amount of PAA produced is calculated based on the volume of NaOH consumed during the first 10 min. This equals the molar amount of 6-APA formed, allowing the enzyme activity of the immobilized PGA to be obtained.

The procedure used to test the activity of the immobilized PGA was as follows. The as-separated immobilized PGA mentioned above was homogeneously mixed with 10 mL deionized water and 5 mL phosphate buffer (0.1 mol/L, pH = 7.8) at 37 °C in a thermostatic bath, and then 30 mL 4% (m/v) aqueous solution of penicillin G potassium salt kept at 37 °C was added. The mixed solution was automatically titrated with NaOH solution (0.1 mol/L) to maintain pH = 7.8, and the volume of NaOH consumed during the first 10 min was measured. The activity of the immobilized PGA was calculated as follows:

$$A \text{ (U/g)} = V_{\text{NaOH}} \cdot C_{\text{NaOH}} \cdot 10^3 / (m \cdot t)$$

where V_{NaOH} is the volume (mL) of NaOH solution consumed, C_{NaOH} is the concentration (mol/L) of the NaOH solution, m is the amount (g) of dry support, and t is the reaction time (min, i.e., 10 min).

The operational stability test was carried out as follows. After testing the initial activity, the solution was separated by centrifugation at 3000 rpm for 5 min, and then the upper water layer was quickly removed. The remnant solid was transferred into a kettle reactor, and its activity was tested by the same method as that mentioned above.

2.6. Characterization

Powder X-ray diffraction (XRD) patterns were collected on a Rigaku D/max-2550VB/PC with Cu K_{α} radiation at 40 kV and 200 mA. N_2 adsorption-desorption isotherms were measured at -196 °C on a Micromeritics ASAP 2020M Sorptometer. Prior to analysis, the functionalized samples were degassed overnight at 110 °C under vacuum, and the unfunctionalized samples were degassed at 350 °C for more than 6 h. The BJH pore size distributions were obtained from the desorption branch of the isotherm using Halsey's thickness equation. Thermogravimetric analyses (TGA) were carried out on a Perkin Elmer thermogravimetric analyzer in air from 30 to 650 °C. Solid state ^{13}C nuclear magnetic resonance (NMR) analysis was performed on a Bruker (Germany) Avance 500 MHz NMR spectrometer. TEM images were obtained on a TECNAI 20S-TWIN electron microscope. Prior to analysis, the samples were dispersed in ethanol by sonication for 20 min and then dropped on a copper grid coated with carbon film.

3. Results and discussion

3.1. Characterization of functionalized CIMS

The XRD patterns of V-CIMS samples and E-CIMS(10%) are shown in Fig. 1. V-CIMS(5%) exhibited two diffraction peaks at $2\theta = 1.41^\circ$ and 1.65° , indicating its hexagonal $p6mm$ structure. These two diffraction peaks disappeared, and a shoulder peak arose at $2\theta = 0.98^\circ$ with increasing amount of VTES in the synthesis solution, which indicated the transformation of the

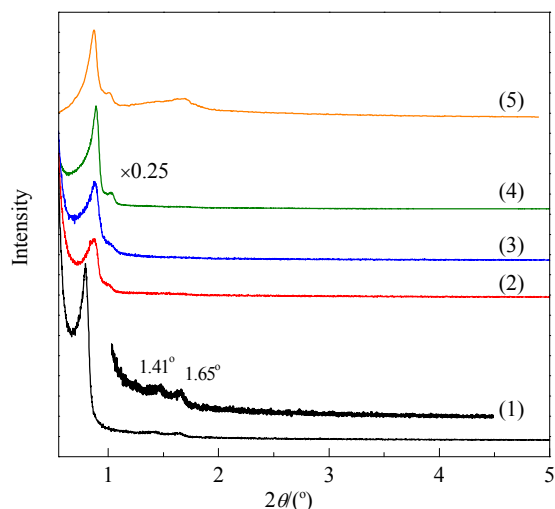


Fig. 1. XRD patterns of V-CIMS(5%) (1), V-CIMS(10%) (2), V-CIMS(15%) (3), V-CIMS(20%) (4), and E-CIMS(10%) (5).

mesoporous structure from the hexagonal $p6mm$ structure to the cubic $Im3d$ phase. In the case of V-CIMS(20%), the cubic $Im3d$ phase was fully developed. These results agree well with the results reported in the literature [37,38], confirming the successful synthesis of vinyl functionalized CIMS.

As shown in Fig. 1(5), E-CIMS(10%) exhibited three diffraction peaks at $2\theta = 0.97^\circ$, 1.11° , and 1.78° , indicating that the cubic $Im3d$ structure was maintained during the epoxidation. TEM images of V-CIMS(10%) and E-CIMS(10%) are shown in Fig. 2. The ordered pore arrays could be clearly observed in the TEM images of both samples, which further confirmed that the epoxidation did not destroy the mesostructure of CIMS.

The N_2 adsorption-desorption isotherms of V-CIMS(10%) and E-CIMS(10%) are shown in Fig. 3. The isotherm of V-CIMS(10%) exhibited the typical type IV isotherms of mesoporous materials with a sharp ramp in the relative pressure range of 0.6–0.8, caused by the capillary condensation of N_2 in the pores [49]. Similarly, the isotherm of E-CIMS(10%) also showed the characteristic step of the isotherm of V-CIMS(10%), and the capillary condensation step appeared in the same relative pressure range. However, the isotherm of PGA/E-CIMS(10%) exhibited almost a straight line (not shown), indicating that the vast majority of the pores of the E-CIMS was filled with PGA. The textural properties of V-CIMS(10%) and E-CIMS(10%) are listed in Table 1. The BET surface area, pore size,

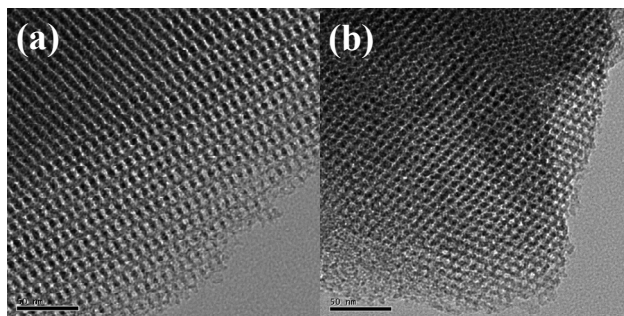


Fig. 2. TEM images of V-CIMS(10%) (a) and E-CIMS(10%) (b).

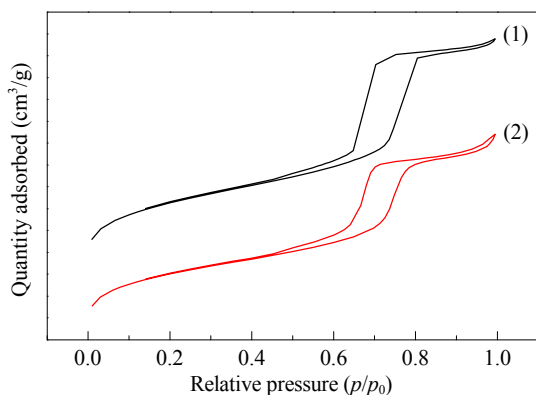


Fig. 3. Nitrogen adsorption-desorption isotherms of V-CIMS(10%) (1) and E-CIMS(10%) (2).

Table 1

Textural properties of V-CIMS(10%) and E-CIMS(10%).

Sample	Surface area (m ² /g)	Pore volume (cm ³ /g)	Pore size (nm)
V-CIMS(10%)	548	0.73	7.1
E-CIMS(10%)	537	0.71	6.9

and pore volume of V-CIMS(10%) were close to those of E-CIMS(10%), indicating that the epoxidation process hardly influenced the mesoporous structure of V-CIMS(10%). This was because the epoxidation of the vinyl groups did not increase or decrease the carbon chains of the organic groups on the surface of the CIMS.

Fig. 4 shows the pore size distributions of the E-CIMS samples, which were all very narrow. However, the pore size of E-CIMS decreased with increasing amount of epoxy groups. The average pore size of E-CIMS(5%) was 7.2 nm, while that of E-CIMS(20%) was 6.2 nm.

Fig. 5 shows the TG curves of as-synthesized V-CIMS(10%) and V-CIMS(10%) after the removal of the P123 template. Two mass losses were observed in the TG curve of as-synthesized V-CIMS(10%). The first, from 150 to 240 °C, was attributed to the combustion of the P123 template, while the other from 240

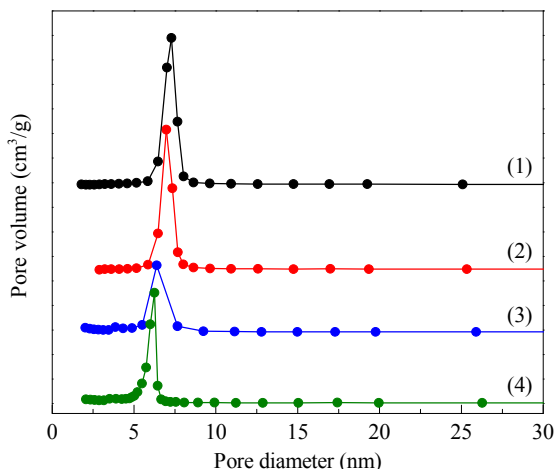


Fig. 4. Pore size distribution curves of E-CIMS(5%) (1), E-CIMS(10%) (2), E-CIMS(15%) (3), and E-CIMS(20%) (4).

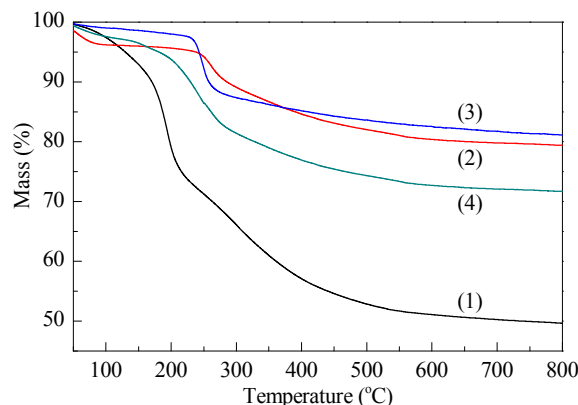


Fig. 5. TG curves of as-synthesized V-CIMS(10%) (1), V-CIMS(10%) after the removal of P123 template (2), E-CIMS(20%) (3), and PGA/E-CIMS(20%) (4).

to 450 °C was attributed to the combustion of P123 template remaining inside the sample and the vinyl groups. However, there was only one mass loss (from 250 to 400 °C) in the TG curve of V-CIMS(10%), which was assigned to the combustion of P123 template remaining in the sample and the vinyl groups. Therefore, the TG results indicated that the majority of the P123 template had been removed from as-synthesized V-CIMS(10%) by the acid treatment.

TG curves of E-CIMS(20%) and PGA/E-CIMS(20%) are also shown in Fig. 5. E-CIMS(20%) had a remarkable mass loss at 210–300 °C, which was attributed to combustion of the epoxy groups on the surface of CIMS and remaining P123 template. Compared with E-CIMS(20%), the PGA/E-CIMS(20%) exhibited much greater mass loss due to the combustion of the immobilized PGA and organic functional groups grafted on the surface of the E-CIMS(20%). These results indicated that the PGA enzyme had been immobilized on the E-CIMS(20%) support.

The solid state ¹³C NMR spectrum of as-synthesized V-CIMS(20%) is shown in Fig. 6. Three resonance peaks at 162.2, 70.1, and 16.2 ppm were observed. The resonance peaks at 70.1 and 16.2 ppm were attributed to the carbon of the P123 template. Comparing the ¹³C NMR of as-synthesized V-CIMS(20%) with that of VTES, the resonance peak at 162.2 ppm was assigned to the carbons of vinyl groups on as-synthesized V-CIMS(20%), indicating the successful incorporation of vinyl groups on the surface of this sample. However, the chemical shift of the carbons in the vinyl groups of as-synthesized

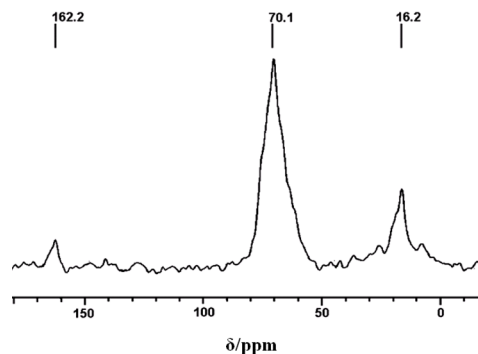


Fig. 6. Solid state ¹³C NMR spectrum of as-synthesized V-CIMS(20%).

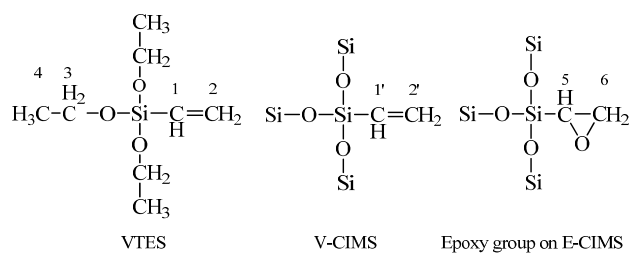


Fig. 7. Scheme of VTES and epoxy group on the surface of E-CIMS.

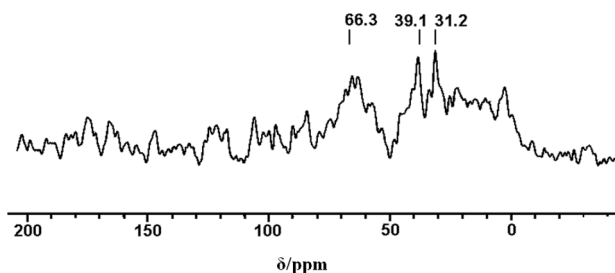


Fig. 8. Solid state ^{13}C NMR spectrum of E-CIMS(20%).

V-CIMS ($\text{C}_{1'}$ and $\text{C}_{2'}$ of V-CIMS in Fig. 7) was moved to higher field, which was attributed to their different chemical environment. Most importantly, the vinyl groups of as-synthesized V-CIMS were in a solid state while the vinyl groups of VTES were in a liquid state.

The solid state ^{13}C NMR spectrum of E-CIMS(20%) is shown in Fig. 8. Three resonance peaks at 66.3, 39.1, and 31.2 ppm were present. The resonance peaks at 39.1 and 31.2 ppm were attributed to the carbons of the epoxy groups on E-CIMS, indicating the successful epoxidation of the vinyl groups of V-CIMS(20%). The resonance peak at 66.3 ppm was attributed to the carbons of remaining P123 template, as shown in the TG results (Fig. 5). These P123 template agents were probably located in the micropores of CIMS and were thus very difficult to extract with H_2SO_4 .

3.2. Performance of immobilized PGA

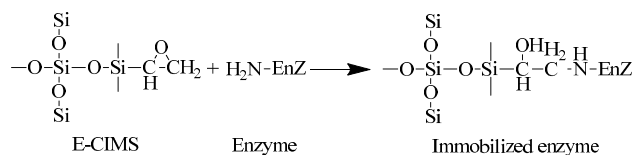
Table 2 shows the enzyme loading, initial activity, and operational stability of PGA immobilized on E-CIMS. The initial activity of the immobilized PGA was found to be lower than that of the free enzyme (13200 U/g). The enzyme loading and the initial activity of PGA/E-CIMS decreased with increasing amount of epoxy groups. There were two reasons for this phenomenon. The decrease in the pore size of E-CIMS blocked PGA

Table 2

Enzyme loading, initial activity, and operational stability of immobilized PGA.

Sample	PGA loading (mg/g)	Initial activity (U/g)	Ratio ^a	Operational stability ^b (%)
PGA/E-CIMS(5%)	209	3611	0.274	76.5
PGA/E-CIMS(10%)	125	2262	0.171	79.9
PGA/E-CIMS(15%)	77	1563	0.118	65.6
PGA/E-CIMS(20%)	63	1308	0.099	63.4

^a Ratio of the initial activity of immobilized PGA to that of the free enzyme. ^b Ratio of the activity of immobilized PGA after five uses to its initial activity.



Scheme 2. Enzyme immobilization on E-CIMS.

molecules from entering into the channels, resulting in fewer PGA molecules immobilized on the support and a corresponding decrease in the initial activity of PGA/E-CIMS. In addition, the incorporation of epoxy groups on CIMS may increase the hydrophobicity of its surface [16,50,51], which was unfavorable for the contact of water-soluble PGA and reaction substrate with E-CIMS, leading to the decrease in the initial activity of immobilized PGA.

The operational stability of PGA/E-CIMS is also shown in Table 2. The operational stability initially increased with increasing amount of epoxy groups on the E-CIMS surface and then decreased with the further increase in the amount of epoxy groups. PGA/E-CIMS(10%) exhibited the highest operational stability, achieving 79.7% of its initial activity after five cycles. Compared with E-CIMS(5%), the E-CIMS(10%) sample possessed more epoxy groups, which enhanced the interaction of E-CIMS support and PGA through chemical bonding (Scheme 2), leading to the improved operational stability of the E-CIMS(10%) sample. However, with further increase in the amount of epoxy groups on the E-CIMS surface, i.e., E-CIMS(15%) and E-CIMS(20%) samples, the pore size and pore volume of the E-CIMS was greatly decreased, which blocked PGA molecules from entering the channels of the CIMS. As a result, more PGA molecules were immobilized on the external surface of E-CIMS or inside channels but near the channel opening. These PGA molecules could be easily washed off during the biocatalytic process, resulting in decreased operational stability of the PGA/E-CIMS.

4. Conclusions

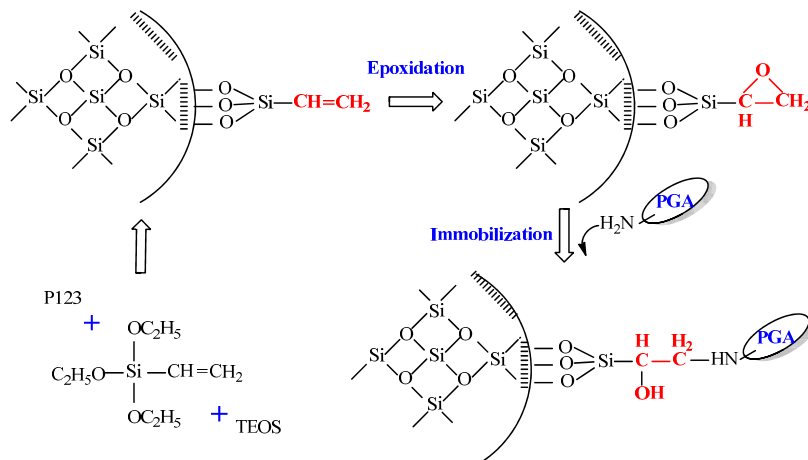
Vinyl functionalized cubic *Ia3d* mesoporous silica was successfully synthesized by co-condensation, and the vinyl groups were epoxidized to prepare epoxy functionalized cubic *Ia3d* mesoporous silica (E-CIMS). The obtained E-CIMS was used as the support for the immobilization of PGA. The enzyme loading of PGA/E-CIMS(5%) was 209 mg/g and its initial activity was 3611 U/g. The enzyme loading and the initial activity of the immobilized PGA decreased with increasing amount of epoxy groups. However, the operational stability of PGA/E-CIMS increased with the amount of epoxy groups on the E-CIMS surface and then decreased with further increases in the amount of epoxy groups. PGA/E-CIMS(10%) exhibited the highest operational stability, achieving 79.7% of its initial activity after five uses. This work therefore provides an efficient way to improve the operational stability of immobilized enzymes. However, it would be preferable to use mesoporous materials with larger pore size and pore volume to enhance the interaction between the epoxy groups and the enzyme.

Graphical Abstract

Chin. J. Catal., 2014, 35: 1709–1715 doi: 10.1016/S1872-2067(14)60156-X

Epoxidation of vinyl functionalized cubic Ia3d mesoporous silica for immobilization of penicillin G acylase

Wangcheng Zhan, Yongjun Lü, Ling Yang, Yanglong Guo, Yanqin Wang, Yun Guo, Guanzhong Lu*
East China University of Science and Technology



Vinyl functionalized mesoporous silica was synthesized and the vinyl groups were epoxidized to prepare epoxy functionalized mesoporous silica, which is an effective support for the immobilization of enzyme through chemical bonding.

References

- [1] Bornscheuer U T. *Angew Chem Int Ed*, 2003, 42: 3336
- [2] DiCosimo R, McAuliffe J, Poulouse A J, Bohlmann G. *Chem Soc Rev*, 2013, 42: 6437
- [3] Katchalski-Katzir E, Kraemer D M. *J Mol Catal B*, 2000, 10: 157
- [4] Cao L Q. *Curr Opin Chem Biol*, 2005, 9: 217
- [5] An Z, He J, Lu S, Yang L. *AIChE J*, 2010, 56: 2677
- [6] Liese A, Hilterhaus L. *Chem Soc Rev*, 2013, 42: 6236
- [7] Liu X H, Bu C H, Nan Z H, Zheng L C, Qiu Y, Lu X Q. *Talanta*, 2013, 105: 63
- [8] He J, Song Z H, Ma H, Yang L, Guo C X. *J Mater Chem*, 2006, 16: 4307
- [9] Yiu H H P, Wright P A. *J Mater Chem*, 2005, 15: 3690
- [10] Hartmann M. *Chem Mater*, 2005, 17: 4577
- [11] On D T, Desplandier-Giscard D, Danumah C, Kaliaguine S. *Appl Catal A*, 2001, 222: 299
- [12] Hartmann M, Jung D. *J Mater Chem*, 2010, 20: 844
- [13] Kim J, Grate J W, Wang P. *Chem Eng Sci*, 2006, 61: 1017
- [14] Chong A S M, Zhao X S. *Appl Surf Sci*, 2004, 237: 398
- [15] Yiu H H P, Wright P A, Botting N P. *J Mol Catal B*, 2001, 15: 81
- [16] Wight A P, Davis M E. *Chem Rev*, 2002, 102: 3589
- [17] Ispas C, Sokolov I, Andreescu S. *Anal Bioanal Chem*, 2009, 393: 543
- [18] Stein A, Melde B J, Schroden R C. *Adv Mater*, 2000, 12: 1403
- [19] Burkett S L, Sims S D, Mann S. *Chem Commun*, 1996: 1367
- [20] Macquarrie D J. *Chem Commun*, 1996: 1961
- [21] Hoffmann F, Cornelius M, Morell J, Froba M. *Angew Chem Int Ed*, 2006, 45: 3216
- [22] Lim M H, Stein A. *Chem Mater*, 1999, 11: 3285
- [23] Sakaguchi K, Matsui M, Mizukami F. *Appl Microbiol Biotechnol*, 2005, 67: 306
- [24] Miyahara M, Vinu A, Ariga K. *J Nanosci Nanotechnol*, 2006, 6: 1765
- [25] Sheldon R A, van Pelt S. *Chem Soc Rev*, 2013, 42: 6223
- [26] Sayari A, Hamoudi S. *Chem Mater*, 2001, 13: 3151
- [27] Huh S, Wiench J W, Yoo J C, Pruski M, Lin V S Y. *Chem Mater*, 2003, 15: 4247
- [28] MacLachlan M J, Asefa T, Ozin G A. *Chem-Eur J*, 2000, 6: 2507
- [29] Wang J, Zou Y C, Sun Y, Hengesberg M, Shffner D, Gao H C, Song X J, Zhang W X, Jia M J, Thiel W R. *Chin J Catal*, 2014, 35: 532
- [30] Cai W J, Zhou Y, Bao R L, Yue B, He H Y. *Chin J Catal*, 2013, 34: 193
- [31] Richer R. *Chem Comm*, 1998: 1775
- [32] Hoffmann F, Cornelius M, Morell J, Froba M. *J Nanosci Nanotechnol*, 2006, 6: 265
- [33] Mateo C, Fernandez-Lorente G, Abian O, Fernandez-Lafuente R, Guisan J M. *Biomacromolecules*, 2000, 1: 739
- [34] Bollner T, Meier C, Menzler S. *Org Process Res Dev*, 2002, 6: 509
- [35] Lü Y J, Lu G Z, Wang Y Q, Guo Y L, Guo Y, Zhang Z G, Wang Y S, Liu X H. *Adv Funct Mater*, 2007, 17: 2160
- [36] Xue P, Xu F, Xu L D. *Appl Surf Sci*, 2008, 255: 1625
- [37] Wang Y Q, Zibrowius B, Yang C M, Spliethoff B, Schüth F. *Chem Commun*, 2004: 46
- [38] Wang Y Q, Yang C M, Zibrowius B, Spliethoff B, Linden M, Schüth F. *Chem Mater*, 2003, 15: 5029
- [39] Xia L Y, Zhang M Q, Rong M Z, Xu W M. *Phys Chem Chem Phys*, 2010, 12: 10569
- [40] Schwartz N N, Blumbergs J H. *J Org Chem*, 1964, 29: 1976
- [41] Asefa T, Kruk M, MacLachlan M J, Coombs N, Grondey H, Jaronic M, Ozin G A. *Adv Funct Mater*, 2001, 11: 447
- [42] Pang J B, Hampsey J E, Hu Q Y, Wu Z W, John V T, Lu Y F. *Chem Commun*, 2004: 682
- [43] Ryoo R, Joo S H, Kim J M. *J Phys Chem B*, 1999, 103: 7435
- [44] Kleitz F, Choi S H, Ryoo R. *Chem Commun*, 2003: 2136
- [45] Xue P, Lu G Z, Guo Y L, Wang Y S, Guo Y. *J Mol Catal B*, 2004, 30: 75
- [46] Yang C M, Zibrowius B, Schüth F. *Chem Commun*, 2003: 1772
- [47] Yang C M, Zibrowius B, Schmidt W, Schüth F. *Chem Mater*, 2004, 16: 2918
- [48] Yang C M, Smatt J H, Zibrowius B, Linden M. *New J Chem*, 2004, 28:

- 1520
- [49] Webb P A, Orr C. Analytical Methods in Fine Particle Technology. Norcross: Micromertics Instrument Corporation, 1997. 53
- [50] Shimada T, Aoki K, Shinoda Y, Nakamura T, Tokunaga N, Inagaki S, Hayashi T. *J Am Chem Soc*, 2003, 125: 4688
- [51] Zhao X S, Lu G Q. *J Phys Chem B*, 1998, 102: 1556